Article:

Seeds, AJ, Fice, MJ, Balakier, K et al. (11 more authors) (2013) Coherent terahertz photonics. Optics Express, 21 (19). 22988 - 23000. ISSN 1094-4087

https://doi.org/10.1364/OE.21.022988

Coherent terahertz photonics

Alwyn J. Seeds,[1] Martyn J. Fice,[1] Katarzyna Balakier,[1] Michele Natrella,[1] Oleg Mitrofanov,[1] Marco Lamponi,[2] Mourad Chtioui,[2] Frederic van Dijk,[2] Michael Pepper,[1,3] Gabriel Aeppli,[3] A. Giles Davies,[4] Paul Dean,[4] Edmund Linfield,[4] and Cyril C. Renaud[1]

[1]*UCL Electronic and Electrical Engineering, Torrington Place, London WC1E 7JE, UK*
[2]*III-V Laboratory, 1, avenue Augustin Fresnel, RD128 F-91767 Palaiseau Cedex, France*
[3]*London Centre for Nanotechnology, Gordon Street, London WC1H 0AH, UK*
[4]*School of Electronic and Electrical Engineering, University of Leeds, Leeds LS2 9JT, UK*
*a.seeds@ ucl.ac.uk

Abstract: We present a review of recent developments in THz coherent systems based on photonic local oscillators. We show that such techniques can enable the creation of highly coherent, thus highly sensitive, systems for frequencies ranging from 100 GHz to 5 THz, within an energy efficient integrated platform. We suggest that such systems could enable the THz spectrum to realize its full applications potential. To demonstrate how photonics-enabled THz systems can be realized, we review the performance of key components, show recent demonstrations of integrated platforms, and give examples of applications.

OCIS codes: (040.0040) Detectors; (040.2840) Heterodyne; (040.5160) Photodetectors; (060.1660) Coherent communications; (110.6795) Terahertz imaging; (140.5965) Semiconductor lasers, quantum cascade; (250.0250) Optoelectronics.

References and links

1. A. G. Davies and E. H. Linfield, eds., "Special Supplement: THz Technology," Electron. Lett. **46**(26), (2010).
2. S. J. Savory, "Digital filters for coherent optical receivers," Opt. Express **16**(2), 804–817 (2008).
3. H. Eisele, "480GHz oscillator with an InP Gunn device," Electron. Lett. **46**(6), 422–423 (2010).
4. L. Moeller, J. Federici, and K. Su, "THz wireless communications: 2.5 Gb/s error-free transmission at 625 GHz using a narrow-bandwidth 1 mW THz source," XXXth URSI General Assembly and Scientific Symposium (2011).
5. C. C. Renaud, M. Robertson, D. Rogers, R. Firth, P. J. Cannard, R. Moore, and A. J. Seeds, "A high responsivity, broadband waveguide uni-travelling carrier photodiode," Proc. SPIE **61940**, 61940C, 61940C-8 (2006).
6. E. Rouvalis, C. C. Renaud, D. G. Moodie, M. J. Robertson, and A. J. Seeds, "Traveling-wave uni-traveling carrier photodiodes for continuous wave THz generation," Opt. Express **18**(11), 11105–11110 (2010).
7. B. S. Williams, S. Kumar, Q. Hu, and J. L. Reno, "High-power terahertz quantum-cascade lasers," Electron. Lett. **42**(2), 89–91 (2006).
8. C. C. Renaud, L. Ponnampalam, F. Pozzi, E. Rouvalis, D. Moodie, M. Robertson, and A. J. Seeds, "Photonically enabled communication systems beyond 1000 GHz," International Topical Meeting on Microwave Photonics (MWP) 2008, 55–58 (2008).
9. R. J. B. Dietz, M. Gerhard, D. Stanze, M. Koch, B. Sartorius, and M. Schell, "THz generation at 1.55 µm excitation: six-fold increase in THz conversion efficiency by separated photoconductive and trapping regions," Opt. Express **19**(27), 25911–25917 (2011).
10. C. Sydlo, M. Feiginov, T. Goebel, D. Schoenherr, P. Meissner, and H. L. Hartnagel, "Electro-optical THz phase control," Conference on Lasers and Electro-Optics (CLEO) 2011 (2011).
11. P. Gellie, S. Barbieri, J. F. Lampin, P. Filloux, C. Manquest, C. Sirtori, I. Sagnes, S. P. Khanna, E. H. Linfield, A. G. Davies, H. Beere, and D. Ritchie, "Injection-locking of terahertz quantum cascade lasers up to 35GHz using RF amplitude modulation," Opt. Express **18**(20), 20799–20816 (2010).
12. M. Ravaro, V. Jagtap, C. Manquest, P. Gellie, G. Santarelli, C. Sirtori, S. P. Khanna, E. H. Linfield, and S. Barbieri, "Spectral properties of THz quantum-cascade lasers: frequency noise, phase-locking and absolute frequency measurement," J. Infrared Milli. Terahz. Waves **34**(5–6), 342–356 (2013).
13. P. Shen, N. J. Gomes, P. A. Davies, and W. P. Shillue, "Generation of 2 THz span optical comb in a tunable fiber ring based optical frequency comb generator," International Topical Meeting on Microwave Photonics (MWP) 2007, 46–49 (2007).
14. M. Kourogi, T. Enami, and M. Ohtsu, "A monolithic optical frequency comb generator," IEEE Photon. Technol. Lett. **6**(2), 214–217 (1994).

#193913 - $15.00 USD Received 16 Jul 2013; revised 11 Sep 2013; accepted 11 Sep 2013; published 23 Sep 2013

15. M. Endo, "Optical frequency comb generator using a single-sideband suppressed-carrier modulation in an amplified circulating fiber loop," Laser Phys. **12**(4), 679–683 (2002).
16. C. C. Renaud, M. Pantouvaki, S. Gregoire, I. Lealman, P. Cannard, S. Cole, R. Moore, R. Gwilliam, and A. J. Seeds, "A monolithic MQW InP/InGaAsP-based comb generator," IEEE J. Quantum Electron. **43**(11), 998–1005 (2007).
17. N. C. Wong, "Proposal for a 10-THz precision optical frequency comb generator," IEEE Photon. Technol. Lett. **4**(10), 1166–1168 (1992).
18. K. Kikuchi, C.-E. Zah, and T.-P. Lee, "Amplitude-modulation sideband injection locking characteristics of semiconductor lasers and their application," J. Lightwave Technol. **6**(12), 1821–1830 (1988).
19. R. T. Ramos and A. J. Seeds, "Fast heterodyne optical phase-lock loop using double quantum well laser diodes," Electron. Lett. **28**(1), 82–83 (1992).
20. A. C. Bordonalli, C. Walton, and A. J. Seeds, "High-performance phase locking of wide linewidth semiconductor lasers by combined use of optical injection locking and optical phase-lock loop," J. Lightwave Technol. **17**(2), 328–342 (1999).
21. L. Ponnampalam, M. J. Fice, F. Pozzi, C. C. Renaud, D. C. Rogers, I. F. Lealman, D. G. Moodie, P. Cannard, C. Lynch, L. Johnston, M. J. Robertson, R. Cronin, L. Pavlovic, L. Naglic, M. Vidmar, and A. J. Seeds, "Monolithically integrated photonic heterodyne system," J. Lightwave Technol. **29**(15), 2229–2234 (2011).
22. K. Balakier, M. J. Fice, C. C. Renaud, L. Ponnampalam, and A. J. Seeds, "Tuneable monolithically integrated photonic THz heterodyne system," International Topical Meeting on Microwave Photonics (MWP) 2012, 286–289 (2012).
23. L. Ponnampalam, R. J. Steed, M. J. Fice, C. C. Renaud, D. C. Rogers, D. G. Moodie, G. D. Maxwell, I. F. Lealman, M. J. Robertson, L. Pavlovic, L. Naglic, M. Vidmar, and A. J. Seeds, "A compact tunable coherent terahertz source based on an hybrid integrated optical phase-lock loop," International Topical Meeting on Microwave Photonics (MWP) 2010, 151–154 (2010).
24. A. J. Ward, D. J. Robbins, G. Busico, E. Barton, L. Ponnampalam, J. P. Duck, N. D. Whitbread, P. J. Williams, D. C. J. Reid, A. C. Carter, and M. J. Wale, "Widely tunable DS-DBR laser with monolithically integrated SOA: Design and performance," IEEE J. Sel. Top. Quantum Electron. **11**(1), 149–156 (2005).
25. S. Ristic, A. Bhardwaj, M. J. Rodwell, L. A. Coldren, and L. A. Johansson, "Heterodyne locking of an integrated optical phase-locked loop," International Topical Meeting on Microwave Photonics (MWP) 2009 (2009).
26. K. Balakier, M. J. Fice, L. Ponnampalam, C. C. Renaud, and A. J. Seeds, "Tuneability of monolithically integrated optical phase lock loop for THz generation," International Topical Meeting on Microwave Photonics (MWP) 2013 (2013).
27. F. van Dijk, M. Lamponi, M. Chtioui, F. Lelarge, G. Kervella, E. Rouvalis, C. C. Renaud, M. J. Fice, and G. Carpintero, "Heterodyne millimeter wave source with monolithically integrated UTC photodiodes," International Topical Meeting on Microwave Photonics (MWP) 2013 (2013).
28. E. Rouvalis, M. Chtioui, F. van Dijk, F. Lelarge, M. J. Fice, C. C. Renaud, G. Carpintero, and A. J. Seeds, "170 GHz uni-traveling carrier photodiodes for InP-based photonic integrated circuits," Opt. Express **20**(18), 20090–20095 (2012).
29. J. Van Rudd and D. Mittleman, "Influence of substrate-lens design in terahertz time-domain spectroscopy," J. Opt. Soc. Am. B **19**(2), 319–329 (2002).
30. R. Mueckstein, C. Graham, C. C. Renaud, A. J. Seeds, J. A. Harrington, and O. Mitrofanov, "Imaging and analysis of THz surface plasmon polariton waves with the integrated sub-wavelength aperture probe," J. Infrared Milli. Terahz. Waves **32**(8–9), 1031–1042 (2011).
31. M. Natrella, O. Mitrofanov, R. Mueckstein, C. Graham, C. C. Renaud, and A. J. Seeds, "Modelling of surface waves on a THz antenna detected by a near-field probe," Opt. Express **20**(14), 16023–16031 (2012).
32. E. Rouvalis, C. C. Renaud, D. Moodie, M. J. Robertson, and A. J. Seeds, "Continuous wave terahertz generation from ultra-fast InP-based photodiodes," IEEE Trans. Microw. Theory Tech. **60**(3), 509–517 (2012).
33. E. Rouvalis, M. Chtioui, M. Tran, F. Lelarge, F. van Dijk, M. J. Fice, C. C. Renaud, G. Carpintero, and A. J. Seeds, "High-speed photodiodes for InP-based photonic integrated circuits," Opt. Express **20**(8), 9172–9177 (2012).
34. A. Beling, Z. Li, Y. Fu, H. Pan, and J. C. Campbell, "High power and high linearity photodiodes," IEEE Photonics Conference 2011, 19–20 (2011).
35. V. Rymanov, M. Palandoeken, S. Lutzmann, B. Bouhlal, T. Telkin, and A. Stoehr, "Integrated photonic 71-76 GHz transmitter module employing high linearity double mushroom type 1.55 µm waveguide photodiodes," International Topical Meeting on Microwave Photonics (MWP) 2012, 253–256 (2012).
36. H. J. Song, K. Ajito, Y. Muramoto, A. Wakatsuki, T. Nagatsuma, and N. Kukutsu, "Uni-travelling-carrier photodiode module generating 300 GHz power greater than 1 mW," IEEE Microw. Wirel. Compon. Lett. **22**(7), 363–365 (2012).
37. M. Chtioui, F. Lelarge, A. Enard, F. Pommereau, D. Carpentier, A. Marceaux, F. van Dijk, and M. Achouche, "High responsivity and high power UTC and MUTC GaInAS-InP photodiodes," IEEE Photon. Technol. Lett. **24**(4), 318–320 (2012).
38. S. Preu, G. H. Doehler, S. Malzer, L. J. Wang, and A. C. Gossard, "Tunable continuous wave terahertz photomixer sources and applications," J. Appl. Phys. **109**(6), 061301 (2011).
39. S. Kumar, "Recent progress in terahertz quantum cascade lasers," IEEE J. Sel. Top. Quantum Electron. **17**(1), 38–47 (2011).

#193913 - $15.00 USD Received 16 Jul 2013; revised 11 Sep 2013; accepted 11 Sep 2013; published 23 Sep 2013

40. S. Barbieri, J. Alton, H. E. Beere, J. Fowler, E. H. Linfield, and D. A. Ritchie, "2.9 THz quantum cascade laser operating up to 70 K in continuous wave," Appl. Phys. Lett. **85**(10), 1674–1676 (2004).
41. B. S. Williams, H. Callebaut, S. Kumar, Q. Hu, and J. L. Reno, "3.4-THz quantum cascade laser based on longitudinal-optical-phonon scattering for depopulation," Appl. Phys. Lett. **82**(7), 1015–1017 (2003).
42. H. Luo, S. R. Laframboise, Z. R. Wasilewski, G. C. Aers, H. C. Liu, and J. C. Cao, "Terahertz quantum-cascade laser based on a three-well active module," Appl. Phys. Lett. **90**(4), 041112 (2007).
43. B. S. Williams, "Terahertz quantum-cascade lasers," Nat. Photonics **1**(9), 517–525 (2007).
44. S. Fathololoumi, E. Dupont, C. W. Chan, Z. R. Wasilewski, S. R. Laframboise, D. Ban, A. Mátyás, C. Jirauschek, Q. Hu, and H. C. Liu, "Terahertz quantum cascade lasers operating up to ~ 200 K with optimized oscillator strength and improved injection tunneling," Opt. Express **20**(4), 3866–3876 (2012).
45. M. S. Vitiello, L. Consolino, S. Bartalini, A. Taschin, A. Tredicucci, M. Inguscio, and P. De Natale, "Quantum-limited frequency fluctuations in a terahertz laser," Nat. Photonics **6**(8), 525–528 (2012).
46. M. S. Vitiello and A. Tredicucci, "Tunable emission in THz quantum cascade lasers," IEEE Trans. THz Sci. Technol. **1**(1), 76–84 (2011).
47. N. Jukam, S. S. Dhillon, D. Oustinov, J. Madeo, C. Manquest, S. Barbieri, C. Sirtori, S. P. Khanna, E. H. Linfield, A. G. Davies, and J. Tignon, "Terahertz amplifier based on gain switching in a quantum cascade laser," Nat. Photonics **3**(12), 715–719 (2009).
48. O. Hatem, J. Cunningham, E. H. Linfield, C. D. Wood, A. G. Davies, P. J. Cannard, M. J. Robertson, and D. G. Moodie, "Terahertz-frequency photoconductive detectors fabricated from metal-organic chemical vapor deposition-grown Fe-doped InGaAs," Appl. Phys. Lett. **98**(12), 121107 (2011).
49. E. Rouvalis, M. J. Fice, C. C. Renaud, and A. J. Seeds, "Millimeter-wave optoelectronic mixers based on uni-traveling carrier photodiodes," IEEE Trans. Microw. Theory Tech. **60**(3), 686–691 (2012).
50. H.-J. Song, K. Ajito, A. Hirata, A. Wakatsuki, Y. Muramoto, T. Furuta, N. Kukutsu, T. Nagatsuma, and Y. Kado, "8 Gbit/s wireless data transmission at 250 GHz," Electron. Lett. **45**(22), 1121–1122 (2009).
51. T. Nagatsuma, H. Song, Y. Fujimoto, K. Miyake, A. Hirata, K. Ajito, A. Wakatsuki, T. Furuta, N. Kukutsu, and Y. Kado, "Giga-bit wireless link using 300-400 GHz bands," International Topical Meeting on Microwave Photonics (MWP) 2009 (2009).
52. H. J. Song, K. Ajito, Y. Muramoto, A. Wakatsuki, T. Nagatsuma, and N. Kukutsu, "24 Gbit/s data transmission in 300 GHz band for future terahertz communications," Electron. Lett. **48**(15), 953–954 (2012).
53. G. Ducournau, P. Szriftgiser, D. Bacquet, A. Beck, T. Akalin, E. Peytavit, M. Zaknoune, and J. F. Lampin, "Optically power supplied Gbit/s wireless hotspot using 1.55 µm THz photomixer and heterodyne detection at 200 GHz," Electron. Lett. **46**(19), 1349–1350 (2010).
54. M. J. Fice, E. Rouvalis, C. C. Renaud, and A. J. Seeds, "1 Gb/s wireless link at 200 GHz using heterodyne detection," IEEE International Microwave Symposium (IMS) 2012 (2012).
55. S. Koenig, F. Boes, D. Lopez-Diaz, J. Antes, R. Henneberger, R. Schmogrow, D. Hillerkuss, R. Palmer, T. Zwick, C. Koos, W. Freude, O. Ambacher, I. Kallfass, and J. Leuthold, "100 Gbit/s wireless link with mm-wave photonics," Optical Fiber Communication Conference (OFC) 2013, paper PDP5B.4 (2013).
56. S. Koenig, J. Antes, D. Lopez-Diaz, I. Kallfass, T. Zwick, C. Koos, W. Freude, and J. Leuthold, "High-speed wireless bridge at 220 GHz connecting two fiber-optic links each spanning up to 20 km," Optical Fiber Communication Conference (OFC) 2012, paper OM2B.1 (2012).
57. P. Dean, Y. L. Lim, A. Valavanis, R. Kliese, M. Nikolić, S. P. Khanna, M. Lachab, D. Indjin, Z. Ikonić, P. Harrison, A. D. Rakić, E. H. Linfield, and A. G. Davies, "Terahertz imaging through self-mixing in a quantum cascade laser," Opt. Lett. **36**(13), 2587–2589 (2011).
58. A. Valavanis, P. Dean, Y. L. Lim, R. Alhathlool, M. Nikolić, R. Kliese, S. P. Khanna, D. Indjin, S. J. Wilson, A. D. Rakić, E. H. Linfield, and A. G. Davies, "Self-mixing interferometry with terahertz quantum cascade lasers," IEEE Sens. J. **13**(1), 37–43 (2013).
59. G. W. Morley, M. Warner, A. M. Stoneham, P. T. Greenland, J. van Tol, C. W. M. Kay, and G. Aeppli, "The initialization and manipulation of quantum information stored in silicon by bismuth dopants," Nat. Mater. **9**(9), 725–729 (2010).
60. P. T. Greenland, S. A. Lynch, A. F. G. van der Meer, B. N. Murdin, C. R. Pidgeon, B. Redlich, N. Q. Vinh, and G. Aeppli, "Coherent control of Rydberg states in silicon," Nature **465**(7301), 1057–1061 (2010).
61. W. K. Hew, K. J. Thomas, M. Pepper, I. Farrer, D. Anderson, G. A. C. Jones, and D. A. Ritchie, "Incipient formation of an electron lattice in a weakly confined quantum wire," Phys. Rev. Lett. **102**(5), 056804 (2009).

1. Introduction

The terahertz (THz) frequency region of the electromagnetic spectrum (0.1 THz – 10 THz) has shown enormous potential for a broad range of applications from health care to security, with communications, high resolution imaging (e.g. in the medical and pharmaceutical sectors), spectroscopic materials analysis and atmospheric sensing of special importance [1]. However, to date, realization of this potential has been severely constrained by the technologies available for the generation and detection of THz signals, which are limited in terms of cost, compactness, energy consumption and room temperature operation. The most

#193913 - $15.00 USD Received 16 Jul 2013; revised 11 Sep 2013; accepted 11 Sep 2013; published 23 Sep 2013

widely available commercial systems are based on broadband THz generation using short pulse (fs) near-infrared lasers and photoconductive detector technology resulting in large, power hungry (kW) systems that have nonetheless helped in demonstrating the potential of THz radiation for spectroscopy and high resolution 3D imaging, thanks to the time discrimination enabled by the short pulse system. However the realisation of the full potential of the THz part of the electromagnetic spectrum will require the use of more agile sources in combination with coherent techniques. As a comparable example, the development of the radio frequency (RF) and microwave spectrum was made possible by the compactness, precision, spectral efficiency and sensitivity enabled by coherent techniques. In recent years coherent technology has also found renewed application in optical communication systems, where it permits the increase in spectral efficiency required to accommodate the rapid growth in internet traffic within the limited optical bandwidth available with current optical amplifiers [2].

We assert that the introduction of coherent photonic technology, based on that used for optical communications, into THz systems will unlock the potential of this part of the frequency spectrum for both scientific and commercial applications. Such a development has, however, long been prevented by the lack of cheap, compact, spectrally pure and power efficient continuous wave sources. Semiconductor electronic sources above 300 GHz currently offer only very low (few μW) output powers, the current room temperature operation record being 86 μW at 479 GHz from a third-harmonic mode InP Gunn effect device with a power consumption of up to 20 W [3], although lower frequency sources followed by diode multipliers have achieved 1 mW output power at 625 GHz [4].

By contrast, the use of photonic technologies would enable the creation of compact, optical fibre interfaced, coherent continuous wave (CW) THz sources, on-chip sensors and receivers, offering unprecedentedly narrow linewidth and concommitantly improved detection sensitivity, with power consumption below 1 W, two orders of magnitude lower than current electronic solutions. Photonic THz sources are based around component technologies such as waveguide Uni-Travelling Carrier Photo-Diodes (UTC-PDs), providing world record, room temperature, CW output powers at THz frequencies [5, 6] and Quantum Cascade Lasers (QCLs) capable of CW output powers of >100 mW [7]. In order to achieve the required coherence these elements must be driven by a photonic heterodyne generator used as the common local oscillator [8]. For reception, detectors can be driven by a similar photonic local oscillator, providing the required coherence for the system, and thus enabling high sensitivity detection. In this paper we will describe in detail the concept of the system as well as its expected performance. We will also show the recent progress made for each of the components to permit the agility, signal power and detection sensitivity that are necessary for system realisation. Finally, we will discuss a few examples of applications and give some recent results demonstrating that the system philosophy presented in the paper has the potential to enable major growth in THz applications.

2. System description

The basic philosophy of the system is shown in Fig. 1. At the heart of the system, a high-purity photonic local oscillator based on optical comb generation and locking of two slave lasers generates an optical heterodyne signal at frequencies ranging from 100 GHz to 5 THz. Such a source enables heterodyne linewidths of considerably less than 10 Hz [8]. The heterodyne signal can then be detected directly in an UTC-PD or an InP-based photoconductive switch [9] to generate a high purity THz signal. Such a system will also enable linewidths five orders of magnitude smaller than the heterodyne systems that have already been used successfully for spectroscopy [10], thus enabling a system with a 50 dB higher signal-to-noise ratio (SNR) if using the lowest possible detection bandwidth.

For frequencies above 2 THz, where, despite the enhanced detection sensitivity, the power emitted (tens of nW) will come close to the noise floor, we propose to use QCLs as emitters

#193913 - $15.00 USD Received 16 Jul 2013; revised 11 Sep 2013; accepted 11 Sep 2013; published 23 Sep 2013

as they are able to offer much higher powers (mW). QCLs can then be locked to the heterodyne generator by an approach similar to that described in [11] or [12], enabling the same coherence as with the photodetection approach together with the enhanced detection described previously.

Such a system is highly dependent on the performance of each of its components. This is reviewed in the next section and the effect on overall system performance described.

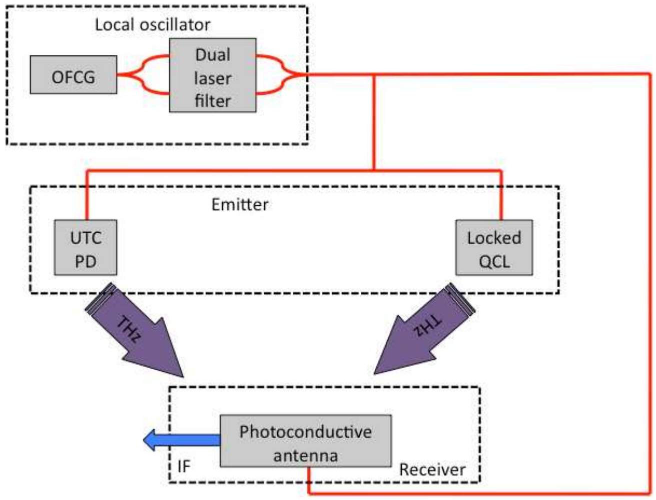

Fig. 1. Schematic of the THz coherent system including the local oscillator, emitter and receiver.

3. Current component performance

The first essential component for the photonic oscillator system is an optical frequency comb generator (OFCG) used as phase reference. Several techniques have been developed over recent years and compact sources are now available [13–16], either fiber or semiconductor based. For example, a system based on the fiber recirculating loop can offer over a hundred highly coherent lines, which are equally spaced in frequency, as determined by an external synthesizer. Figure 2 shows optical spectra of an OFCG and two semiconductor lasers for selection of two comb lines (spaced by the frequency of interest). The comb optical lines are defined within a 7dB power envelope across 2 THz range and could be further amplified if necessary.

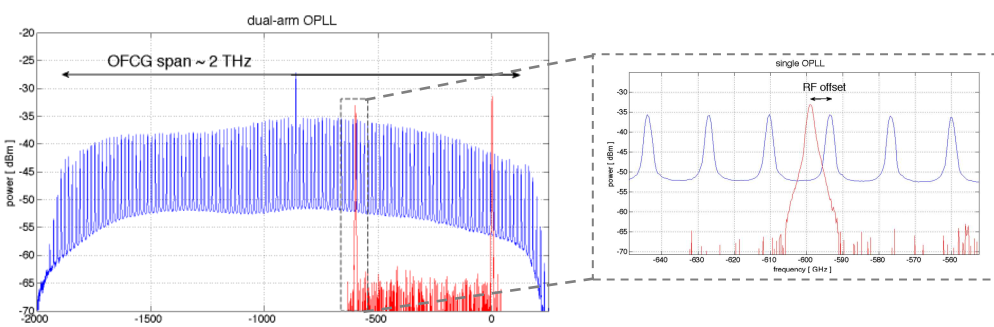

Fig. 2. Optical spectrum of the OFCG (in blue) and the 800 GHz heterodyne signal between two tuneable lasers (in red).

The best performing OFCG of that type, as proposed in [17], should offer up to 10 THz in span, using parametric methods, with several mW of total output power, while short pulse mode locked lasers have achieved similar performances. Compact sources have achieved up to 2 THz span [13] with similar power. Current performance is therefore close to what will be needed for the system, as only a few mW will be required to lock the slave lasers and a span of 5THz will be sufficient to access most applications.

The second important part of the system is the dual-laser locked filter, whose principal function is to select and amplify the comb lines of interest. This can be realized using methods such as optical injection, optical phase lock loops (OPLL) and optical injection phase lock loops (OIPLL) [18–20]. Figure 3 presents the block diagram of the heterodyne OPLL system and the operating principle is broadly discussed in [21, 22].

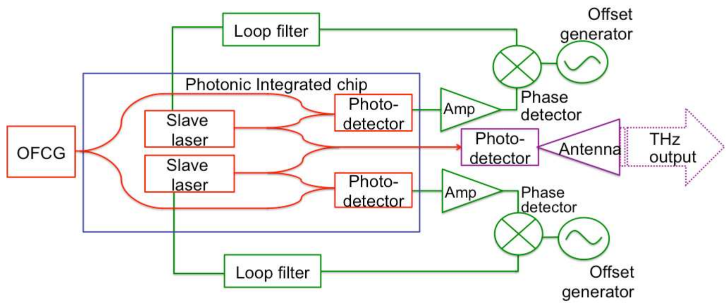

Fig. 3. Schematic of the integrated photonic heterodyne OPLL THz source. Red lines correspond to optical components. Green lines correspond to electrical paths and components.

Recent work in the development of dual laser sources has seen great progress. Integrated sources with tuning up to a 2 THz frequency difference have been demonstrated [23], while tuneable lasers with tuning ranges of more than 5 THz are already available [24]. The semiconductor lasers offer an important advantage in terms of device lifetime, compactness and efficiency. On the other hand, they have a less coherent output, with linewidth in the lower MHz range. To phase lock the source successfully with such a large linewidth, individual components incorporated in the OPLL must have bandwidth in the range of hundreds of MHz. Consequently, this requires the error signal to be fed back around the loop with delays on a nanosecond timescale to achieve locking. To ensure superior loop performance, the trade off between laser linewidth or loop bandwidth and inversely proportional loop propagation delay must be satisfied. The OPLL with nanosecond propagation delay remains highly challenging and can be realized only thanks to a compact high-speed electronic circuit and monolithically integrated photonics. Despite difficulties, recent developments have shown great progress in achieving integrated phase lock loop circuits such as in [25] and [21].

The photonic local oscillator based on OPLL enables heterodyne linewidth of less than 10 Hz and phase noise performance better than −80 dBc/Hz at 10 kHz offset across the frequency range, as shown in Fig. 4(a) and 4(b) respectively. Dual laser locked sources have shown discrete tuning over a range of more than 1 THz with continuous tuning with an offset of 2 to 6 GHz at both sides of the comb line of interest [22, 26].

#193913 - $15.00 USD Received 16 Jul 2013; revised 11 Sep 2013; accepted 11 Sep 2013; published 23 Sep 2013

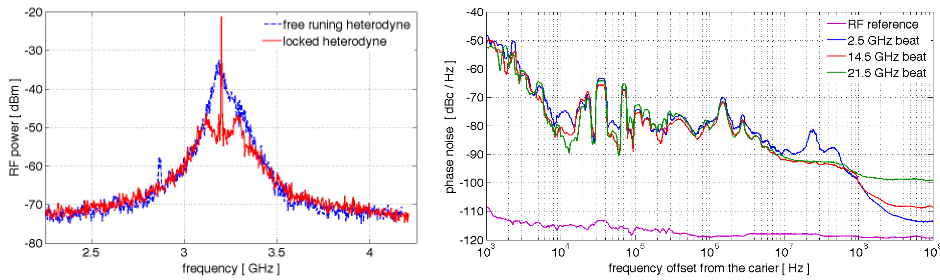

Fig. 4. (a) Beat note spectra at 2.5 GHz (RBW = 100 kHz, VBW = 10 kHz); (b) phase noise measurement of the phase locked heterodyne signal at 2.5 GHz, 14.5 GHz and 21.5 GHz.

Integrating the high-speed photodetector used for THz generation with the dual laser source is an important goal, as it avoids fiber coupling between separate modules, simplifying fabrication and reducing cost. However, it is technically challenging, as the epitaxial structures required for the laser and photodetector sections are significantly different. We have recently integrated dual laser sources with UTC-PDs achieving emission at frequencies exceeding 60 GHz [27] as shown in Fig. 5, which also emphasizes the importance of the correct selection of substrate doping. For the results shown in Fig. 5, the maximum frequency was limited by the measurement probe, but discrete photodetectors with the same structure exhibited bandwidths up to 170 GHz [28].

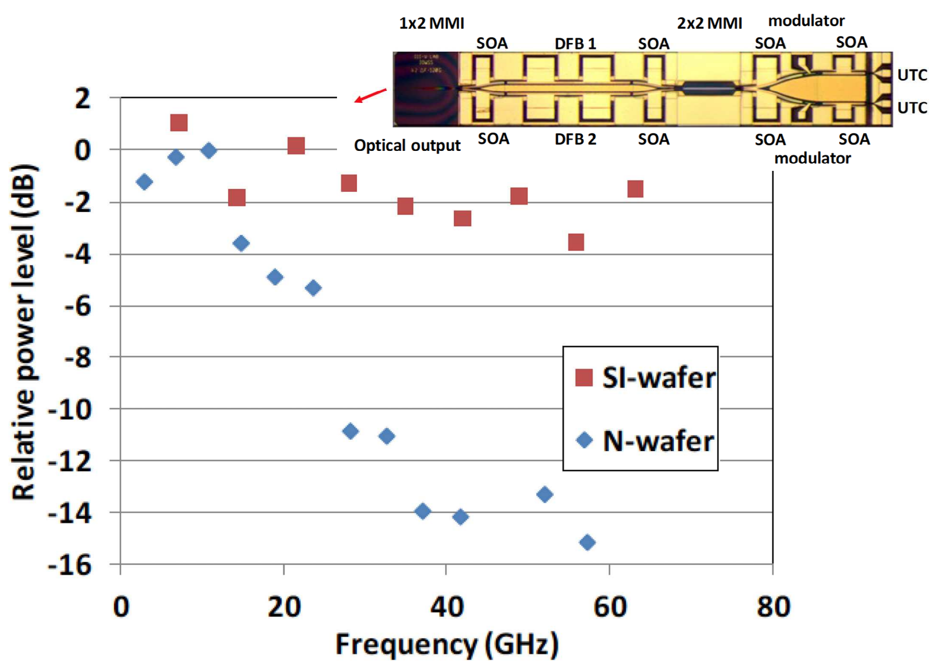

Fig. 5. Relative output power from an integrated UTC PD with dual DFB lasers at different frequencies [27] SI: Semi Insulating; N: N doped.

Conversion of the photocurrent in photodiodes into free-space THz radiation is typically realized by integrating the UTC-PDs with a planar antenna, such as a dipole, bow-tie, spiral or log-periodic antenna, and a silicon lens. In order to exploit the tuneability of photonic THz sources, the integrated THz antenna must have a wide bandwidth, both in terms of the efficiency of energy coupling from the driving source and in terms of the radiation pattern and radiation efficiency. Assessment of the reflection coefficient between the driving source (typically a UTC-PD) and the antenna is complex and needs to be carried out case by case depending on the source employed. Conversely, the radiation pattern and radiation efficiency are intrinsic properties of antennas and can be evaluated independently from the source.

Emission pattern and radiation efficiency of planar THz antennas tend to change dramatically over the frequency range of UTC-PDs. Therefore silicon lenses are typically employed to improve the beam shape and radiation efficiency. Figure 6 illustrates the effect of the silicon lens attached to the antenna substrate on the radiation pattern. When the lens is not present, the substrate modes and reflections occurring within the substrate cause the emission pattern to change almost unpredictably as a function of frequency. The integration of the lens provides good and broadband focusing properties that produce several dBi in directivity over a wide frequency range. Figure 7 shows the radiation efficiency (in dB) calculated in the conical solid angle centered on the axis origin and defined by an angle of 30 degrees with respect to the z negative semi axis (which corresponds to the optical axis of the lens); above about 0.250 THz, the radiation efficiency of the system with lens is greater than or at least equal to the maximum radiation efficiency of the system without lens at 0.5 THz. The peak of the radiation efficiency without lens occurring at 0.5 THz is probably due to a fortunate favorable recombination of the reflections within the substrate and the antenna response. The fact that the radiation efficiency with the lens tends on average to improve as the frequency increases can be explained considering that THz lenses are usually designed and optimized using ray optics (geometrical optics); the ray optics approximation becomes more accurate as the frequency goes up (smaller wavelength) therefore the lens design and optimization is more accurate at higher frequencies. The chip-lens configuration that we have simulated can be considered as a collimating hemisphere design where the distance from the emitter to the tip of the lens is about 1.4 times the lens radius [29].

Antennas are also used for detection of THz radiation. To improve the detection efficiency, the antenna is used to couple the incoming THz wave to the small area of the photodiode, the active area of which is significantly smaller than the wavelength. As in the case of THz emitters, the antenna design affects the conversion efficiency. In addition to numerical modelling, the antenna performance can be evaluated experimentally using near-field THz imaging [30, 31].

For the emitters, UTC-PDs have already shown record-breaking figures of merit for conversion of light to THz signals up to 1.6 THz [32]. As shown in Fig. 8, the figure of merit remains high across the range. The integrated double laser/UTC-PD sources described above have shown potential for use in a simple emitter chip [27], while UTC-PD devices from the chip were tested as stand-alone detectors, showing a 3dB bandwidth of >100 GHz [33]. Comparing the UTC-PD with other photodetectors used as photomixers, as shown in Fig. 9, it is evident that UTC-PDs offer the highest power emission performance below 100 GHz, while further analysis shows that higher power extraction has also been achieved at THz frequency [6, 30–38]. They are therefore attractive THz sources for systems applications.

#193913 - $15.00 USD Received 16 Jul 2013; revised 11 Sep 2013; accepted 11 Sep 2013; published 23 Sep 2013

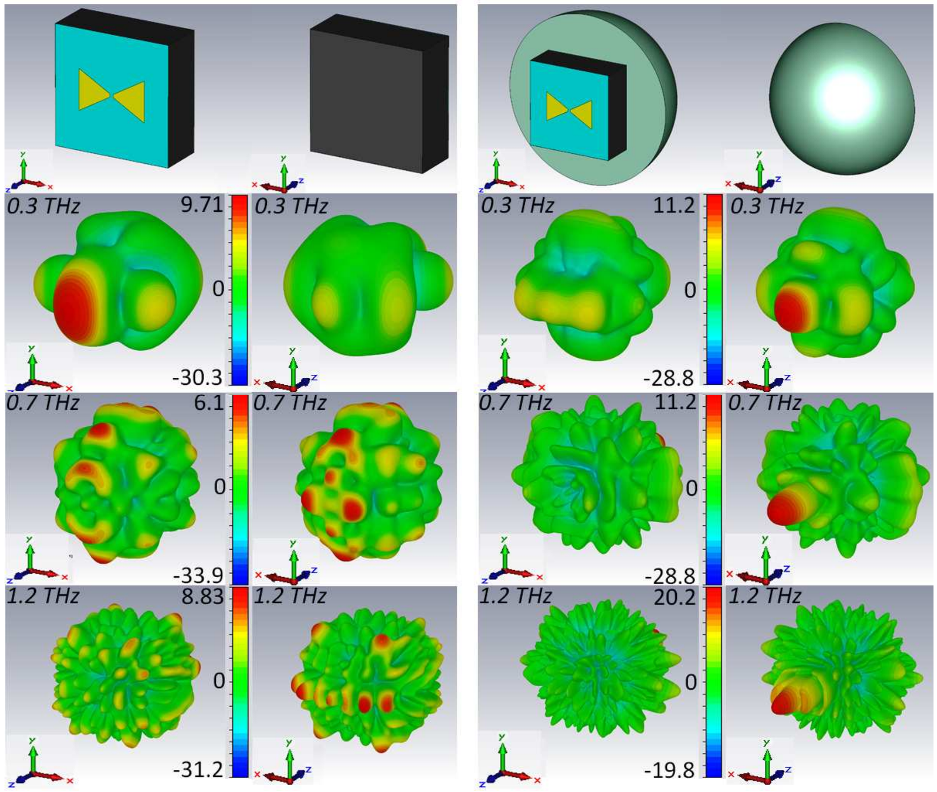

Fig. 6. Directivity in dBi. The bow-tie antenna is 600 µm long and has a 60° angle. The InP substrate is 400 µm thick. The silicon lens has a 2 mm diameter.

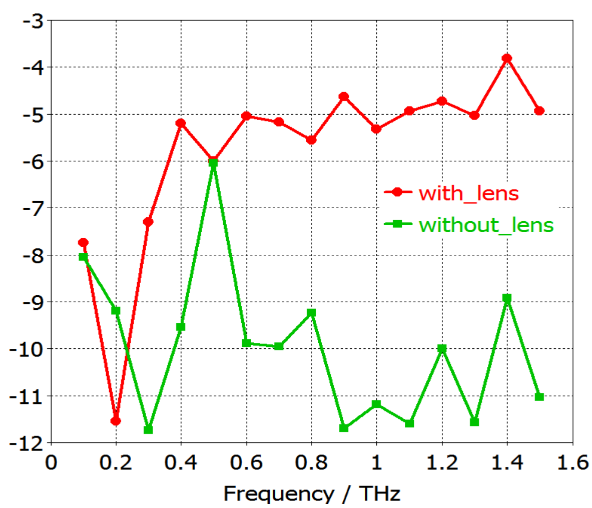

Fig. 7. Radiation efficiency in dB calculated in the conical solid angle centered on the axis origin and defined by an angle of 30° with respect to the z negative semi axis.

#193913 - $15.00 USD Received 16 Jul 2013; revised 11 Sep 2013; accepted 11 Sep 2013; published 23 Sep 2013

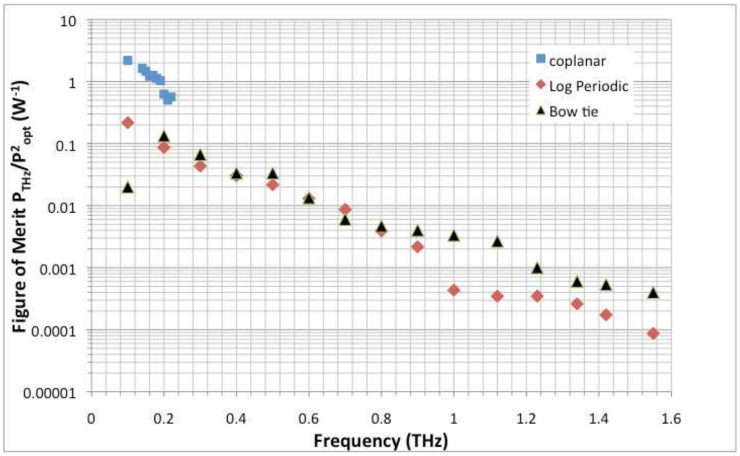

Fig. 8. Figure of merit of UTC-PD emitters from 100 GHz to 1.6 THz.

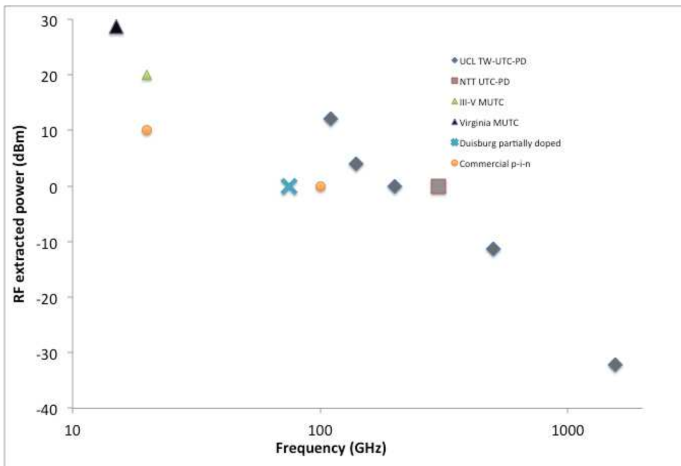

Fig. 9. Recent examples of record output power as a function of frequency for UTC-PDs compared to other photodetectors [6, 32–37].

Meanwhile progress on QCL sources has been considerable over the past ten years and power output is now >100 mW [7], with emission frequencies ranging between 1 and 5 THz having been demonstrated [39]. Central to these advances has been the design and engineering of a range of active region schemes, most notably the bound-to-continuum (BTC) [40] and resonant-phonon (RP) [41, 42] designs. The latter exploits fast electron–optical-phonon scattering to depopulate the lower lasing level – an approach that enables a population inversion to be maintained up to high operating temperatures, at which thermal backfilling [43] of the lower lasing state prevents operation of alternative active region schemes. As such the temperature of operation of QCL devices has increased to approaching 200K [44]. Nevertheless, owing to the requirement to drop > 36 meV (the LO phonon energy in GaAs) across each individual module of the RP structure, large applied biases are required at threshold. This leads to large electrical power dissipation in RP QCLs, making continuous wave operation challenging. The BTC design, which typically exhibits low threshold current densities, is therefore most frequently employed for applications requiring continuous wave operation. Lasers based on such a design have also recently been shown to exhibit intrinsic linewidth values approaching the quantum limit [45], and as such are well-suited to the

#193913 - $15.00 USD Received 16 Jul 2013; revised 11 Sep 2013; accepted 11 Sep 2013; published 23 Sep 2013

development of coherent systems. Tuneable QCL devices have been demonstrated using a range of approaches [46] together with electronic control using multi-contact lasers [47].

Devices for coherent THz detection have also shown significant progress in recent years. Both Schottky mixer and LT-GaAs photoconductors are enabling good performance over different parts of the frequency range. For compatibility with the photonic components emitting at a wavelength of 1.5 μm, implanted InGaAs switches [48] and quantum well based switches [9] show great promise to be used as a detector in the system. Similarly, considering the integration potential, recent results on optically pumped mixing in UTC-PDs offer an interesting solution, despite their current relatively high conversion loss [49].

4. Demonstration

As mentioned in the introduction, a number of applications have been envisaged for THz technology. In this section we concentrate on a few examples where the development of the proposed system would help realize the potential of the THz spectrum.

First, one can look at wireless communication where current technology at lower carrier frequencies is limited by the available licensed bandwidth. However, in the unlicensed spectrum above 300 GHz the bandwidth available would easily allow for a transmission rate of more than 10 Gb/s. Recent results for THz wireless links employing photonic carrier generation at frequencies ranging from 200 GHz to 400 GHz have indeed demonstrated the possibility of transmitting wireless data at more than 1 Gb/s. Above 250 GHz, detection has been limited to incoherent envelope detection using Schottky barrier diode (SBD) detectors [50–52], but the demonstration of data transmission at up to 28 Gb/s [52] clearly shows the potential for high bandwidth wireless transmission at these carrier frequencies, although, due to transmission impairments and the low signal powers available, a compromise will need to be found between carrier frequency and spectral efficiency.

The coherent system we propose enables the application of classical coherent radio modulation techniques that allow for higher sensitivity and the use of more spectrally efficient modulation formats. Heterodyne detection of a photonically generated 1 Gb/s on-off keying (OOK) modulated signal at 200 GHz has been demonstrated, using a subharmonic SBD mixer for down conversion, and envelope detection of the intermediate frequency (IF) signal [53]. In a similar experiment to demonstrate the key elements of our proposed approach, we used a real-time oscilloscope (RTO) to record samples of the IF signal, and offline processing enabling envelope [54] and synchronous detection to be emulated (Fig. 10). Recently, a wireless link using a photonic heterodyne transmitter operating at a carrier frequency of 237.5 GHz has been demonstrated with QPSK, 8PSK and 16QAM modulation formats at 25 Gbaud, giving up to 100 Gb/s data transmission rates [55]. A monolithic microwave IC (MMIC) I/Q receiver was used to down convert to baseband, followed by analogue-to-digital conversion using a RTO and offline digital signal processing similar to that used in coherent optical receivers. These demonstrations of coherent detection of wireless communications at THz frequencies all employed electronic local oscillators (LOs) generated by frequency multiplication of an RF signal, but in the future the LO could be generated photonically, especially if efficient optoelectronic mixers can be developed. However, the benefits of photonic-enabled THz wireless communications will need to be evaluated in comparison to a fully electronic approach. Already, both transmitter and receiver MMICs supporting data rates up to 20 Gb/s and operating at 220 GHz have been demonstrated [56], while 2.5 Gb/s transmission at 625 GHz has been achieved using electronic frequency multiplication [4].

#193913 - $15.00 USD Received 16 Jul 2013; revised 11 Sep 2013; accepted 11 Sep 2013; published 23 Sep 2013

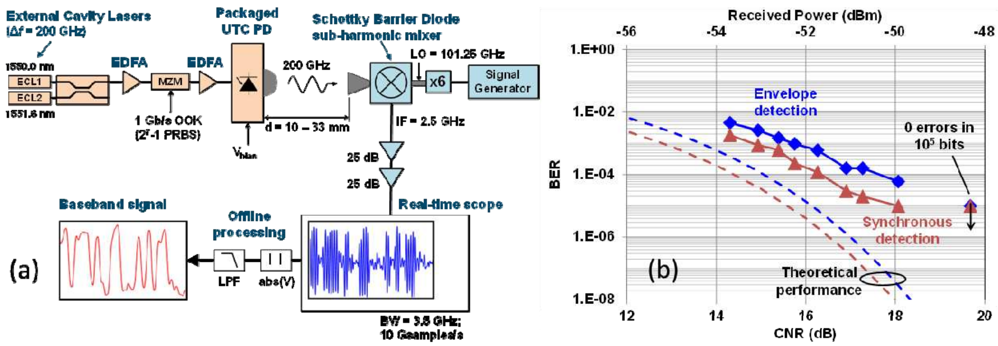

Fig. 10. Demonstration of wireless transmission of 1 Gb/s OOK data at 200 GHz [54]: (a) experimental arrangement; (b) BER results for offline processing emulating envelope and synchronous detection.

A second application would be the development of a simple imaging system based most likely on the QCL source as it offers more power. In this application the coherence of the signal allows the use of interferometric techniques, enabling phase-sensitive and 3D imaging. Recent work on QCL coherent imaging, as illustrated in Fig. 11, has shown encouraging results in imaging different reflective elements [57], showing clear interferometric fringes indicating changes in depth. The experimental system was based on the coherence of the QCL which is typically 5 orders of magnitude worse than the system proposed. In this application an enhanced coherence will allow for better fringe definition and higher resolution as well as higher sensitivity, enabling longer distances for imaging. Indeed, imaging has previously been demonstrated, using this approach, at round-trip distances exceeding 20m through air [58].

Fig. 11. Coherent imaging of a set of objects using a coherent QCL based system [57, 58].

Finally, we would also like to discuss the potential of THz techniques for the measurement and manipulation of quantum states. Typically, microwave measurement and manipulation of quantum states has been achieved using multiple controlled pump pulses and coherent re-emission, which is monitored as a function of pulse length, arrival times, and amplitudes [59]. However, because of the lack of appropriate sources, very few experiments of this type have been performed in the THz regime, though recent experiments using a free electron laser and high frequency microwave sources have demonstrated the potential of THz radiation for

#193913 - $15.00 USD Received 16 Jul 2013; revised 11 Sep 2013; accepted 11 Sep 2013; published 23 Sep 2013

quantum control and measurement, with results already achieved for the Rydberg states of Si:P [60].

The use of a small source which can be inserted directly into a dilution refrigerator will allow the study of transitions between electron interaction induced states such as those observed in the Coulomb Blockade regime. Other aspects of the interaction which we can study include the transition between a single line of electrons and two separate rows which form a many body ground state [61].

Using the coherent THz system we envisage, there is potential for introducing a compact lab-on-chip THz system that will enable control using optical communications-based modulation techniques, offering unprecedented opportunities to study a far wider range of coherent electronic and lattice excitations.

6. Discussion

We have described an approach to the development of a coherent THz system technology, underpinned by photonic components, that would enable access to most applications for frequencies ranging from 100 GHz to 5 THz. Reviewing recent developments in device technology we have shown that the photonic sources necessary to generate a tuneable local oscillator are becoming available, while photonic THz emitter technology has already reached an encouraging state of development, with both UTC-PDs and QCLs offering good performance. We have shown the potential of coherent THz systems to achieve 5 orders of magnitude enhancement in sensitivity and 2 orders of magnitude enhancement in energy consumption relative to pulsed sources, while offering good potential for integration. We have also discussed potential applications for such systems, as well as the potential improvements they enable, allowing for over 100 Gb/s wireless transmission, compact 3D imaging and quantum state manipulation with a lab-on-chip system.

Acknowledgments

This work was supported by Engineering and Physical Sciences Research Council (EPSRC) grants PRINCE (GR/S86631/01), PORTRAIT (EP/D502225/1) and COTS (EP/J017671/1), and by the European Commission through the European project iPHOS (grant agreement no: 257539). We also acknowledge support from the ERC programmes NOTES and TOSCA; the Royal Society and Wolfson Foundation (AGD); and EPSRC Fellowships (PD, EP/J002356/1; EHL, EP/J005282/1).